Future aspects of Vector Meson production at HERA

H. Abramowicz[a], T. Doeker[a1], L. Iannotti[b], S. Kananov[a], A. Levy[a] and L. West[c]

[a] School of Physics and Astronomy, Raymond and Beverly Sackler Faculty of Exact Sciences, Tel Aviv University
[b] Physics Department, Calabria University
[c] School of Physics, University of Birmingham

Abstract: The analysis of exclusively produced vector mesons in deep inelastic scattering offers the opportunity for detailed tests of QCD predictions. This report gives an overview of the expected rates for vector meson production and investigates the accuracy which can be achieved with an increase in statistics and a better understanding of the existing detector components of the H1 and ZEUS experiments. Requirements for the HERA luminosity and detector upgrades are described for several vector meson related measurements.

1 Introduction

The study of the exclusive production of vector mesons provides important information on the hadronic structure of the photon and the nature of diffraction. The simplicity of the final state makes this process attractive for almost parameter-free QCD calculations. Several recent QCD based approaches are available to predict the cross section for exclusive vector meson production [1, 2, 3, 4]. These calculations require the presence of a hard scale to be applicable. In addition phenomenological models also give estimates for this process [5]. The comparison of the HERA data with these estimates will help to test those models and to determine the kinematic range in which they are reliable.

The aim of this report is to determine which of the theoretical predictions can be tested by experiment (and in which kinematic range), which accuracy is needed to distinguish between different models and what are the demands for the HERA machine and experiments to perform such measurements. The focus of this work is on the vector meson production at high Q^2 or t.

Throughout this paper we assume that the central detectors of the H1 and the ZEUS experiments are available in their present setup and that the ongoing improvement of the detector understanding will allow to use the full tracking systems of the two experiments. The *forward* components of the detectors are of special interest for the estimate of the proton dissociation contribution to the cross section. The limits to the measurements due to the layout of these components are investigated.

This article is organized as follows: Chapter 2 gives an introduction to the kinematic variables and a brief overview of some QCD models for elastic vector meson production. Based on

[1] Supported by MINERVA

these models, estimates for the rates of exclusively produced vector mesons are given. Chapter 3 describes the detector setup, the expected acceptance in the kinematic range and the expected systematic uncertainties of the measurements. In Chapter 4 the accuracy of future measurements is evaluated. Chapter 5 summarizes the requirements for HERA.

2 Cross section estimates

2.1 Vector meson production at large Q^2

In this section some general aspects of elastic vector meson electro-production,

$$e(k) + p(P) \rightarrow e(k') + V(v) + p(P') \tag{1}$$

will be briefly discussed.

The kinematic variables which are used throughout the paper are defined as follows:

- $Q^2 = -q^2 = -(k-k')^2$,
- $x = \frac{Q^2}{2(P\cdot q)}$,
- $t = (q-v)^2 = (P-P')$,
- $s = (P+k)^2$,
- $y = \frac{q\cdot P}{k\cdot P}$,
- $W = \sqrt{ys}$,

where Q^2 is the negative square of the 4-momentum transfer at the electron vertex, y is the inelasticity parameter, t is the 4-momentum transfer squared between the photon and the vector meson, x is the Bjorken variable, s is the ep center-of-mass energy squared and W is the γ^*p center-of-mass energy.

The ep cross section is related to the $\gamma^*p \rightarrow Vp$ cross section:

$$\frac{d^2\sigma_{tot}(ep \rightarrow eVp)}{dy\ dQ^2} = \Gamma_T\ \sigma_{tot}(\gamma^*p \rightarrow Vp), \tag{2}$$

where Γ_T is the flux of transverse virtual photons given by

$$\Gamma_T = \frac{\alpha_{em}\ (1-y+y^2/2)}{\pi y Q^2}. \tag{3}$$

Hard diffractive electro-production of longitudinally polarized vector mesons has been studied recently in the framework of perturbative QCD [2], where the cross section of the $\gamma^*p \rightarrow Vp$ process was calculated within the leading $\alpha_s \ln \frac{Q^2}{\Lambda^2_{QCD}}$ approximation of QCD using the leading order parton densities within the proton. V denotes any vector meson (e. g. $\rho, \rho', \phi, J/\Psi, \Upsilon$). When the momentum transferred to the target t tends to zero and $Q^2 \gg M_V^2$, where M_V is the vector meson mass, the cross-section for the hard diffractive electro-production has the form:

$$\left.\frac{d\sigma^L_{\gamma^*p\rightarrow Vp}}{dt}\right|_{t=0} = \frac{4\pi^3\Gamma_{V\rightarrow e^+e^-} M_V \alpha_s^2(Q^2) T(Q^2) \eta_V^2 \left| \left(1 + i\frac{\pi}{2}\frac{d}{d\ln x}\right) xG(x,Q^2)\right|^2}{3\alpha_{EM} Q^6}, \tag{4}$$

where $\Gamma_{V\rightarrow e^+e^-}$ is the decay width of the vector meson into an e^+e^- pair. The parameter η_V is defined as $\eta_V \equiv \frac{1}{2}\frac{\int \frac{dz\, d^2k_t}{z(1-z)}\phi_V(z,k_t)}{\int dz\, d^2k_t\, \phi_V(z,k_t)}$, and ϕ_V is the light-cone wave function of the $q\bar{q}$ component of the vector meson. $xG(x,Q^2)$ is the gluon distribution in the proton and $T(Q^2)$ is a factor connected with the Fermi motion of the quarks within the vector meson.

The predictions of pQCD for diffractive electro-production of vector mesons have been partly compared with the existing experimental results [6, 7, 8]:

- A fast increase of the cross section of electro-production of vector mesons with the $\gamma^* p$ center of mass energy W, $\sigma \sim W^{0.8-0.9}$. The rise is connected with the behavior of the gluon density with decreasing x. The non-perturbative two-gluon-exchange model of Donnachie and Landshoff [5] predicts a cross section rising as $\sim W^{0.32}$ which, after taking into account the shrinkage of the forward diffractive peak becomes $\sim W^{0.22}$.

- The dominance of the longitudinal polarization, $\sigma_L/\sigma_T \propto Q^2/M_V^2$.

- The absolute magnitude of the cross section is reasonably well explained, though uncertainties in the knowledge of $xG(x,Q^2)$ are too large to make a quantitative comparison.

- The account of Fermi motion of the quarks within the vector meson leads to a strong suppression of the cross section. The dependence of the suppression factor $T(Q^2)$ on the Q^2 for light and heavy mesons was presented in [2].

- The Q^2 dependence of the cross section can be parameterized as Q^{-n} with $n \sim 4$. The difference of n from the asymptotic value of 6 is changed by the Q^2 dependence of the factors $[\alpha_s(Q^2)xG(x,Q^2)]^2 \sim Q$ and of $T(Q^2)$.

Based on equation (4) with the GRV94 LO gluon distribution [9], we have calculated the cross section[2] for production of longitudinally polarized vector meson states $\sigma_L(\gamma^* p)$ as a function of W for the different ranges of Q^2 for the following vector mesons: $\rho(770)$, $\rho(1700)$, $\phi(1020)$, $J/\psi(3097)$ and $\Upsilon(9460)$. The kinematic ranges were chosen as $20-150$ GeV^2 for Q^2 and 40 - 220 GeV for W. The cross section (4) was integrated over t between $t_{min} = 0$ and $t_{max} = 1$ GeV^2 assuming the e^{bt} behavior of the cross section with slope $b = 5$ GeV^{-2}. The total cross section $\sigma_{tot}(\gamma^* p \to Vp)$ is defined as: $\sigma_{tot}(\gamma^* p \to Vp) = \sigma_L(\gamma^* p \to Vp)(1/R + \varepsilon)$, where ε is the polarization parameter, $\varepsilon = \frac{1-y}{1-y+y^2/2}$, $R = \sigma_L/\sigma_T$, and σ_T is the transverse $\gamma^* p$ cross section.

In fig. 1 the total $(\gamma^* p \to \rho p)$ cross section as a function of energy W is displayed. One can see the predicted [1, 2] strong rise of the cross section with W.
Using the electro-production cross sections we have calculated the expected number of vector mesons N_V:

$$N_V = \sigma(ep \to Vep) \times \mathcal{L} \times \mathrm{Br}; \qquad (5)$$

where $\mathcal{L}$ denotes the integrated luminosity and Br the branching fraction of vector mesons. We have considered the following decay channels : $\rho(770), \rho(1700) \to \pi^+\pi^-$, $\phi \to K^+K^-$, J/Ψ, $\Upsilon \to e^+e^-$ and $\mu^+\mu^-$. The value of $Br = 0.3$ was assumed for $\rho(1700) \to \pi^+\pi^-$ decay.

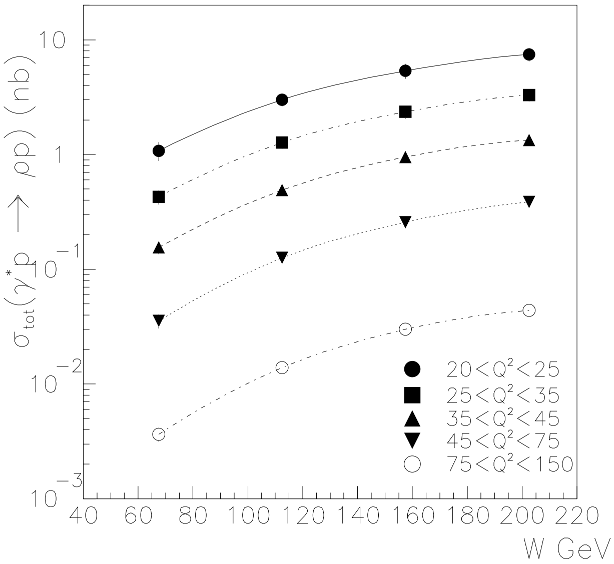

Figure 1: *Predicted cross section of ρ^0 production as function of W and Q^2 [1,2].*

In table 1 the estimated rates of events with $\mathcal{L}$=250 pb^{-1} are displayed. In addition we show in the table the extrapolated number of events for 250 pb^{-1}, based on the currently available event statistics.

[2]In case of heavy mesons production Q^2 was replaced by $Q^2 + M_V^2$.

$Q^2[GeV^2]$	20-25	25-35	35-45	45-70	70-150	Total	$Q^2 > 7\text{GeV}^2$ estim. from data
$\rho(770)$	1100	800	250	170	30	2350	60000
$\phi(1020)$	150	100	40	20	5	315	6000
$\rho(1700)$	17	40	13	11	4	95	-
J/$\psi(3097)$	130	130	60	30	10	360	3000
$\Upsilon(9460)$	1.7	1.6	1.3	0.8	0.5	6	-

Table 1: *Estimated number of events in the measurable W range for different Q^2 ranges. We would like to thank E. Gallo for preparing the estimated number of events from the current data.*

2.2 Vector meson production at large t

The process $\gamma p \to V + X$, where V is a vector meson and X is a hadronic state originated by the diffractive dissociation of the proton (fig. 2(a)), in the limit of large t, has been described in the BFKL formalism in terms of the exchange of a perturbative QCD pomeron [11, 4]. In such a model, the vector meson is produced quasi-elastically, i.e. in the proton rest frame it carries nearly all the energy of the photon. The photon can be either quasi-real ($Q^2 \simeq 0$) or virtual ($Q^2 > 0$).

2.2.1 Kinematics and cross section

In addition to the standard kinematic variables, the model [11, 4] uses two extra variables. These are the scaling variable, τ, and the 'energy' variable z defined as:

$$\tau = \frac{-t}{(Q^2 + M_V^2)} \quad \text{and} \quad z = \frac{3\alpha_s}{2\pi} \log\left(\frac{x_g \cdot W^2}{-t + Q^2 + M_V^2}\right) ,$$

where x_g is the fraction of the proton momentum carried by the struck parton. The variable z is proportional to the rapidity gap between the produced vector meson and the scattered parton. The differential cross section for the process $\gamma p \to VX$, when the photon is transversely polarized, is written as:

$$\frac{d^2\sigma_T(\gamma p \to VX)}{dt dx_g} = \left(G(x_g, t) + \frac{16}{81}\sum_f (q(x_g, t) + \bar{q}(x_g, t))\right) \frac{\pi \alpha_s^4}{t^4} \mid \mathcal{F}(z, \tau) \mid^2 ,$$

where G, q and $\bar{q}$ represent the gluon, quark and anti-quark densities respectively, and $\mathcal{F}$ is the product of the two-gluon scattering amplitude and the form factor associated with the γV vertex [11, 4]. The cross section for longitudinal photons is assumed to be $\sigma_L = (Q^2/M_V^2)\sigma_T$.

2.2.2 Monte Carlo Generators

Two Monte Carlo generators have been written which simulate the large t vector meson production process, named HITVM [15] and RHODI [16]. The available vector mesons are ρ, ω, ϕ, J/ψ or Υ in both generators. However, as a non-relativistic wave function is used in the calculations, the predictions for the ρ, ω and ϕ mesons are not as reliable as for the heavier vector mesons. The two Monte Carlo generators agree in their results for both the γp and ep cross sections. The main difference between the two generators is the modeling of the proton remnant:

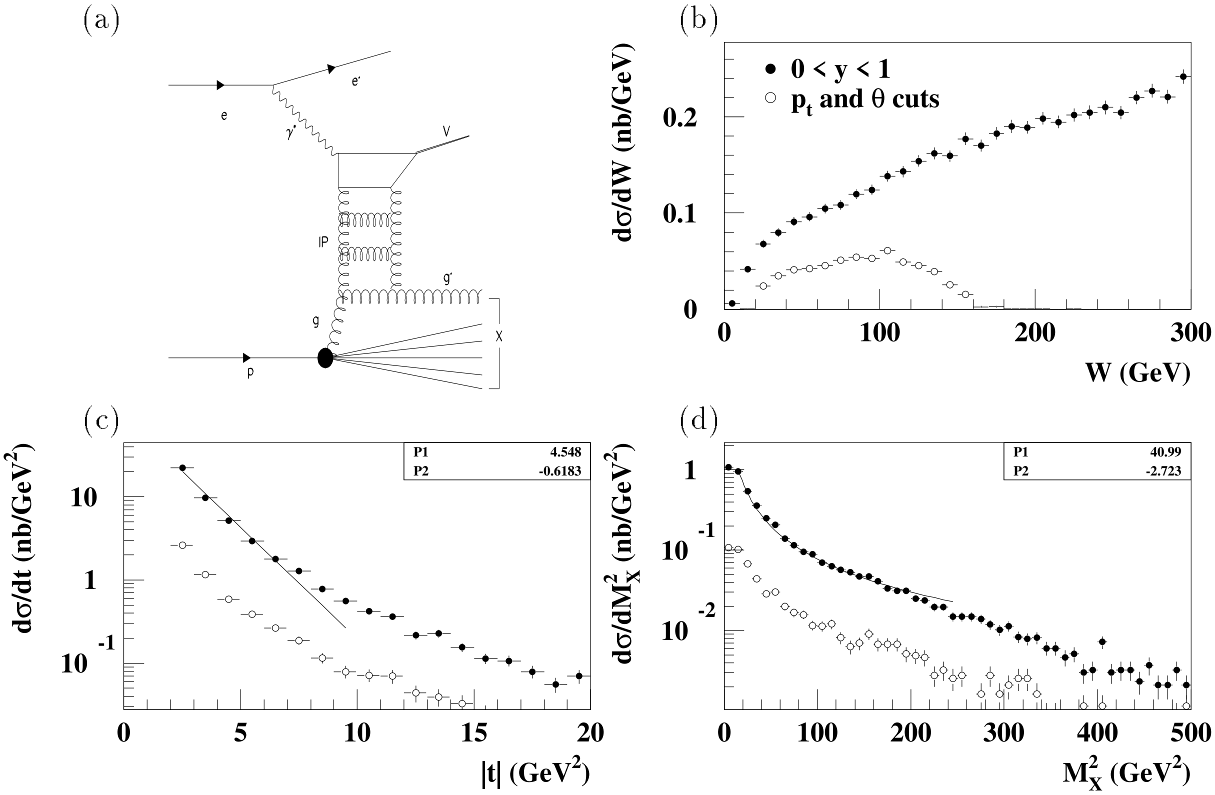

Figure 2: *For the process $ep \to e'VX$ at large t, (a) shows the Feynman diagram, (b) the W distribution, (c) the $|t|$ distribution fitted with $p_1 \cdot e^{\,p_2 t}$ and (d) the M_X^2 distribution fitted with $p_1 \cdot (M_X)^{p_2}$ when $V = J/\psi$. The closed and open circles represent the generated distributions and the distributions after applying the p_t and θ cuts indicated in the text, respectively. For these plots the HITVM generator was used.*

- In RHODI the multiplicity and momentum distribution of the hadrons produced from the proton dissociation are generated using parameterizations of the $\bar{p}p \to \bar{p}(p)X$ results from the UA5 experiment [12] and imposing two requirements on M_X: $M_X^2/W^2 \leq 0.1$ (to ensure that the interaction be diffractive) and $M_X \geq m_p + m_\pi$ (to remove the events with only a proton in the diffractive state X).

- In HITVM, the struck parton can be either a valence quark, gluon or sea quark and in each case the proton remnant is a diquark, quark+diquark or quark+baryon respectively (based on the method used by PYTHIA [13]). Then the resulting particles are given to JETSET [13] to hadronize.

2.2.3 Cross section predictions

Table 2 summarizes the ep cross sections expected for J/ψ production and also the expected number of $J/\psi \to \mu^+\mu^-$ (or e^+e^-) events for a luminosity of $100\,\mathrm{pb}^{-1}$. In order to simulate the apparatus acceptance, events were accepted only if both muons are in the range $6° < \theta < 155°$ and $p_t > 1.0$ GeV. The predictions are calculated in the region $0.01 < x_g < 1.0$, $|t| > 2.0$ GeV^2 and using $\alpha_s = 0.3$ and the structure functions MRSA [14]. The predictions are very sensitive to the value of α_s: for example when $\alpha_s = 0.2$ the cross section is reduced by a factor of 20.

The generated and accepted distributions in W, $|t|$ and M_X^2 for $Q^2 < 4\,\mathrm{GeV}^2$ are shown figures 2(b), 2(c) and 2(d), respectively. Note the strong increase of the cross section with W and that this model predicts a very small W-dependence of the t-slope ($\alpha' < 0.1$ GeV^{-2}).

Kinematic Range	$\sigma(ep \to e'J/\psi X)$ (nb)		$N(J/\psi \to \mu^+\mu^-)$	
	$Q^2 < 4$ GeV^2	$Q^2 > 4$ GeV^2	$Q^2 < 4$ GeV^2	$Q^2 > 4$ GeV^2
$0.000 < y < 1.00$	46.	1.4	250000	8000
$0.015 < y < 0.60$	30.	1.0	150000	6000
$0.010 < y < 0.30$	17.	0.67	100000	4000
Muon p_t and θ cuts	5.90	0.36	35000	2000

Table 2: *Cross section predictions and the expected number of $J/\psi \to \mu^+\mu^-$ events for 100 pb^{-1}.*

3 Detector performance

This study is based on the present layout of the two multi-purpose detectors at HERA H1 and ZEUS. It is assumed that in the near future the full tracking system of both experiments will be available and that during the HERA upgrade no changes to the tracking chambers are needed. The acceptance of the tracking systems of the two detectors is similar. In case of the ZEUS detector the polar coverage of the central drift chamber is $16^o - 165^o$, the forward tracking chambers cover the region $7^o - 28^o$ and the rear tracking system the region $160^o - 170^o$.

Like for the selection of all diffractive processes at HERA, an efficient tagging of very forward particles is needed to distinguish between single and double dissociative events.

The identification of all vector meson decay products and of the scattered electron allows the complete and precise reconstruction of the event kinematics. However, the additional detection of the scattered proton selects an almost proton dissociation free subsample and allows additional important cross checks. Due to the small acceptance of a leading proton spectrometer ($\sim 5\%$), measurements are limited to the low Q^2 region.

More important for future vector meson selections at large Q^2 is the tagging of proton fragments in the very forward region. This method to separate single from double dissociative events has the advantage of high acceptance and is not limited to a small t-region. We will discuss the importance of tagging particles as forward as possible in the context of systematic errors.

We assume for the study that the trigger for the vector meson events will not be a basic problem. The clean topology of the events should help to select such events already in a very early trigger stage.

3.1 Acceptance

The understanding of the detector acceptance increases normally slowly with time. Using the DIPSI Monte Carlo generator [10] we checked with the standard simulation of the ZEUS detector that the average acceptance of vector mesons is above 60% in the relevant W range. For the following we used the simple approximation that the chance to identify a vector meson is high if its original direction is within the acceptance range of the tracking chambers.

Figure 3 shows the pseudo-rapidity ($\eta = -\ln\tan\frac{\theta}{2}$) of the vector mesons as function of W with Q^2 as additional parameter; the dependence of the acceptance on t and M_V is in case of large Q^2 very small. For example using the complete tracking system for $Q^2 = 20$ GeV^2, the

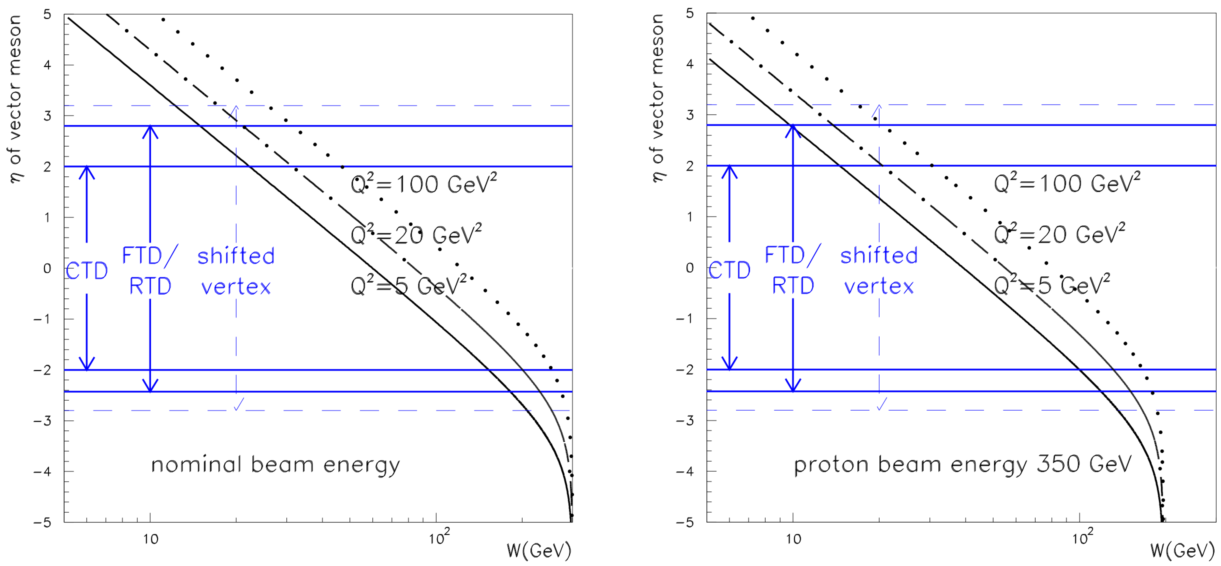

Figure 3: *Rapidity of scattered vector meson as function of W and Q^2 for nominal beam energies (left, E_p = 820 GeV, E_e = 27.5 GeV) and reduced proton energy (right, E_p = 350 GeV). The full lines indicate the acceptance of the tracking chambers. The dashed line shows the acceptance of the full tracking system for shifted vertex runs (±70 cm).*

accepted W range for vector mesons is roughly $25 - 220$ GeV. Additional shifted vertex runs (with z ± 70 cm) can extend the η range by ± 0.4 units and increase the W range slightly.

Changing the proton beam energy to lower values helps to extend the measurements to smaller values (see fig. 3 for a proton beam of 350 GeV). Measurements down to $W = 10$ GeV will be possible and therefore the results of the NMC collaboration can be cross-checked. A change of the electron beam energy does influence the direction of the vector meson only at very large W values, close to the kinematic limit, but it shifts the events to higher values of y. Measurements with a reduced electron beam energy can therefore be used to estimate R, the ratio of transverse to longitudinal cross section, directly, without the assumption of s-channel helicity conservation.

The acceptance as function of Q^2 depends mostly on the layout of the detector responsible for tagging the scattered electron. The main calorimeters of the H1 and ZEUS experiments can be used for this purpose down to Q^2 values of a few GeV^2. Events with smaller Q^2 values can be selected with additional taggers along the beam pipe. For the full reconstruction of the event kinematics at least the measurement of the direction of the scattered electron is required.

3.2 Systematic errors

The systematic uncertainties will become more important for the measurements at high luminosity. The sources of uncertainties can be divided into the following subgroups: reconstruction of the final state particles, non-resonant background, proton-dissociation and other sources like luminosity measurement, radiative corrections, non-physical background. The following estimates are based on the two presently available publications on vector meson production at high Q^2 [7, 8].

1. **Reconstruction:** The present error estimate in the cross section measurements related to uncertainties in the acceptance and the reconstruction of the event kinematic is about 7%. A large effort is underway by both collaborations to get a better determination of

the position of the scattered electron, a better understanding of the track reconstruction efficiency and of the sources of calorimeter noise. This certainly will reduce the systematic error soon. The usage of additional components (tracking chambers in the forward and rear region, new components in the very forward region) will create new sources of uncertainties. Overall a reduction of this error down to 4% should be possible.

2. **Non-resonant background:** Neither the shape of e. g. the resonant ρ-mass peak nor of the underlying non-resonant background is known for the production of vector mesons at large Q^2 values. So far different assumptions about the shape of the non-resonant mass distributions were used to fit the data and to estimate this background source (6%). The higher statistics in future measurements will help to constrain the assumptions about the shape and the fit result. An estimate of 4% seems reasonable.

3. **Proton-dissociation:** With an uncertainty of about 8% the estimate of the contribution of events where the proton dissociates is the largest source for the systematic error. The contribution (and therefore the error estimate) can be reduced either by tagging the outgoing proton or by tagging excited proton states of very low masses. Due to the higher acceptance the second method is favored for the vector meson selection. The main problem for the cross section measurement is the a priori unknown mass-spectrum of the excited proton states.

   Monte Carlo simulations are used to estimate the untagged mass distribution of the proton fragments for different detector layouts. We studied the two cases that the tagging device has an acceptance down to 1.5 mrad or only down to 6 mrad (the lower limit of 1.5 mrad is given by the fact that for a momentum transfer squred (t) on the proton of about 1GeV^2 the proton is scattered by 1.2 mrad!). In the first case, excited states of the proton above 1.8 GeV, while in the second case above 2.2 GeV are rejected. Assuming a mass dependence of the excited proton state $\sim M_N^{-2.0}$ such devices can veto 92% (84%) of the events where the proton dissociates. Assuming the cross section for proton dissociation to be of the same order as for the elastic scattering, the remaining background of about 8% (16%) can be constrained by assumptions about the M_N or t dependence. We assume one half of this contribution as a conservative estimate of the systematic error.

   For the determination of the t-slope, this error leads to an uncertainty of the measured slope of about ± 0.2 GeV^{-2} (± 0.4 GeV^{-2}).

4. **Other sources:** Compared to the errors above, the uncertainties of the luminosity measurement should be negligible and the improved knowledge of the Q^2-dependence will reduce the uncertainties in the calculation of radiative corrections.

The following table summarizes the estimates of systematic errors:

error	93/94	future estimate
reconstruction related	7%	4%
non-resonant background	6%	4%
proton-diss. background tagged at 1.5 / 6 mrad	8%	4% / 8%
other sources	5%	-
	13%	7% / 10%

The overall systematic error is therefore expected to be about 7% (or about 10% if only proton fragments above 6 mrad are tagged). Since the dependence of the background on the kinematic variables is not known, for cross section measurements the error contribution has to be taken into account for each measured bin independently, rather than using an overall normalization uncertainty. In case of the measurement of R, cross section ratios are measured at the same W and Q^2 values (but different y), it can be therefore assumed that the systematic errors partly cancel and a systematic error of 5% is reasonable.

4 Accuracy of measurements

In this section the accuracy is estimated for future measurements related to elastic vector meson production under the assumptions explained previously [3]. We consider the measurement of the power δ of the W-dependence, the change of the t-slope described by the value of α' and the ratio of $\sigma_L/\sigma_T = R$. Different theoretical predictions for these observables are available. The aim of this section is to define the luminosity needed to distinguish between the predictions.

In order to minimize the error of the measurement, some time was spent to optimize the bin sizes. As long as the statistical error dominates, the chosen bin size has almost no influence on the resulting error. If only two or three bins in W are used for the δ and α' measurement, the loss of "lever arm" in W gives a slightly higher error. If the systematic error becomes important, the best results are observed if the bin size is adjusted such that the systematic error is smaller or equal to the statistical error in each bin.

The estimate of the error of the δ and α' measurement is almost independent on the assumed model. Once the W and t range is given by the detector acceptance, the error depends only on the number of events which are available in a given Q^2-interval. Following the ideas of Frankfurt et al. [2], in the range of large Q^2 ($>$ a few GeV^2) the dynamics of vector meson production will vary only slowly with Q^2, thus relatively large bins in Q^2 can be used. See tables 1 and 2 for the expected number of events in the given Q^2 ranges.

4.1 W-dependence

Equidistant W-bins were used and a systematic error of 7% was added to the statistical error in each bin. The resulting error for δ is shown in fig. 4. The lines correspond to the accessible W range at $Q^2 = 20$ GeV^2 if either only the central tracking chambers of the experiments are used or the full tracking systems are available. In the second case with about 100 events in a given Q^2 interval the error on δ is ≈ 0.2. HERA data can therefore very soon discriminate between the very different predictions of e.g. Donnachie-Landshoff and QCD approaches for the ρ meson. With an integrated luminosity of about 250 pb^{-1} this accuracy can be expected for Q^2 values up to 35 GeV^2 also for ϕ and J/ψ mesons. Above 1000 events the systematic error dominates and limits the precision on δ to 0.05. This limit is important at low Q^2 values for ρ, ϕ and J/ψ production.

4.2 α'-measurement

The (non-) observation of "shrinkage" requires a detailed understanding of the t-dependence of the cross section. The slope of the t distribution of proton dissociative events is smaller than the slope of the elastic sample. Therefore proton dissociation becomes important at large t values and limits the accuracy of the measurement of the t-slope.

[3]The following study is done for the elastic vector meson production; however, the results are in principle also valid for the production of vector mesons at large t.

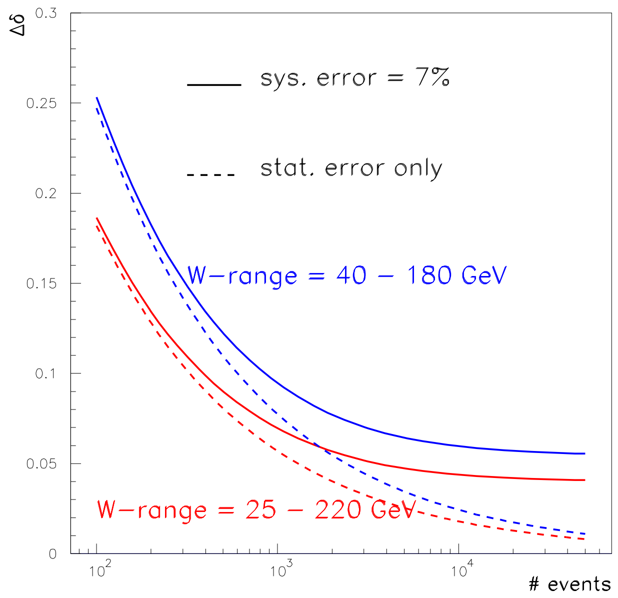

Figure 4: *Estimate of the error for a δ measurement as function of the number of events in a given Q^2 range.*

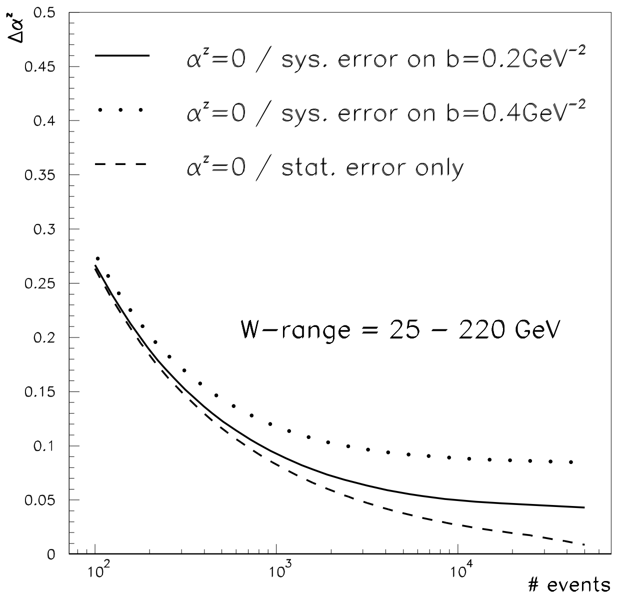

Figure 5: *Estimate of the error for a α' measurement as function of the number of events in a given Q^2 range.*

In each W-bin the statistical error for the t-slope measurement was calculated. We used for the t-fit the range $0.1 - 1.0$ GeV^2. The lower limit is given by the expected beam emittance for the low β optics of HERA, the upper limit by the influence of proton dissociation background. To the statistical error we add the systematic error of $\Delta b = \pm 0.2$ GeV^{-2} (0.4 GeV^{-2}). The error of the α'-fit is shown in fig. 5.

The value of α' in soft physics is about 0.25 GeV^{-2}. To establish that this value is excluded by 2 standard deviations, the error of the measurement should be below 0.12 GeV^{-2}. From fig. 5 it can be seen that at least 1000 events are needed. From table 1 it can be concluded that only the ρ cross section at higher Q^2 values is large enough to enable such a measurement. With a luminosity of 1000 pb^{-1} the requested accuracy can be achieved also for the ϕ and J/ψ mesons at intermediate Q^2 values.

If proton fragments can only be tagged above 6 mrad the resulting error is almost twice as high. It is then impossible to measure α' with the requested accuracy. This result demonstrates very clearly the importance of a good tagging of proton fragments in the very forward region.

4.3 Measurement of R

The measurement of the ratio between the cross section of longitudinally and transversely polarized photons gives additional information about the structure of a virtual photon. Two different approaches are available to measure R: either comparing the cross sections at fixed W and Q^2, but at different beam energies (the ratio of the transverse to the longitudinal photon flux changes with the ep center-of-mass-energy) or assuming s-channel helicity conservation (SCHC) and measuring the helicity distribution of the final state particles.

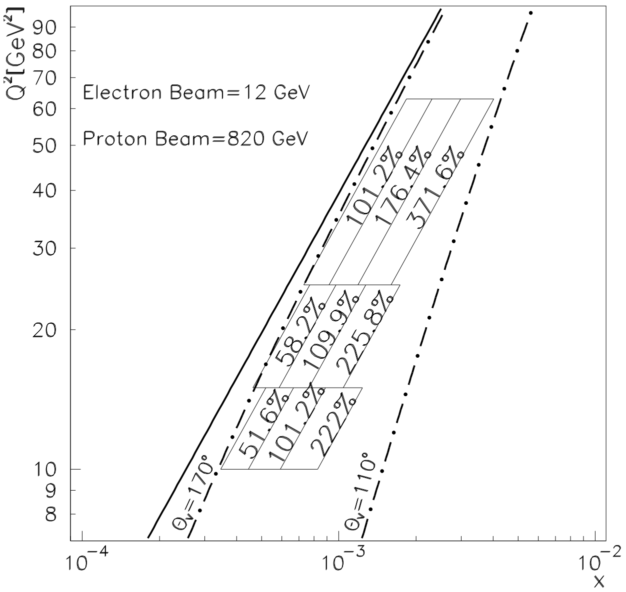

Figure 6: *Error estimate for R. The cross section is measured in the shown W, Q^2-bins at two different electron beam energies (27.5, 12 GeV) with about 10 pb^{-1} luminosity. The dotted lines indicate constant values of the VM scattering angle.*

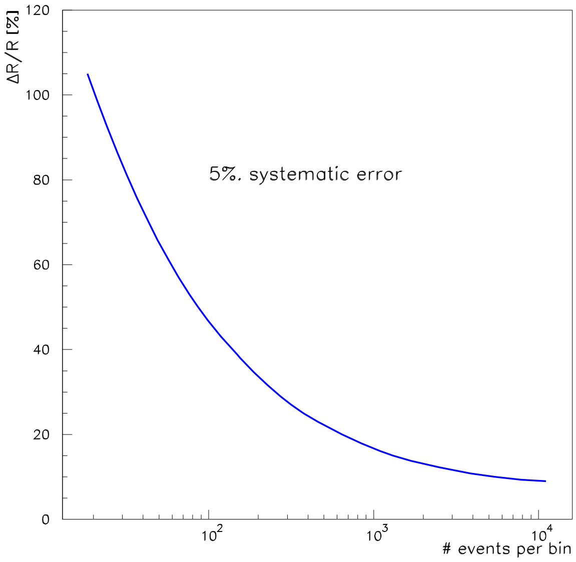

Figure 7: *Error estimate for the measurement of R from the helicity distribution of the final state particles. For the estimate of the systematic uncertainty a flat distributed background with an uncertainty of 5% is assumed.*

4.3.1 Reduced beam energy

At the nominal beam energy, the acceptance of the central tracking limits the measurements of exclusive vector meson production to small and intermediate values of y ($4 \cdot 10^{-3} < y < 0.5$). The transverse and longitudinal photon fluxes differ significantly only at very high y values. The practical way for the selection of vector mesons at high y values is the reduction of the electron beam energy. The error estimate of R for some W- and Q^2- bins is given in fig. 6. For this estimate we used the cross section prediction for the ρ^0-meson of section 2.1, assumed a 5% error between the two cross section measurements at high and low beam energies and considered the case that about 10pb^{-1} are available at each energy. The error, which is mostly of statistical nature, is in all bins above 50%. If 100pb^{-1} are taken at each energy, the error in the highest W-bins is reduced to about 25%.

4.3.2 Assuming SCHC

The helicity distribution of the vector meson decay products contains information about the polarization of the vector meson. If one assumes that the helicity is conserved in the diffractive interaction, the vector meson has the same polarization as the original photon. The fraction of transversely to longitudinally polarized photons can therefore be estimated. The assumption of SCHC has been proven for small values of t and Q^2. But an indication was seen, that this assumption is not true at large values of t [17].

The acceptance for vector mesons is reduced if $\cos(\theta_h)$, θ_h being the polar angle of one decay product of the vector meson in the vector meson c.m. system, is close to ± 1. In that case typically one of the decay particles has only a very small momentum. However, the region of $|\cos(\theta_h)| < 0.8$ is unaffected. The error of a fit to the helicity distribution is plotted in fig.7. The accuracy of this method is better than the one described in 4.3.1. A combination of both methods might be used to check SCHC.

5 Conclusions

The analysis of exclusively produced vector mesons at HERA provides important tests of QCD predictions. Significant differences exists in the predictions between phenomenological and perturbative QCD models. We concentrate in this report on the QCD predictions available at large values of t and Q^2. We studied the requirements for the HERA accelerator and the two experiments H1 and ZEUS to enable measurements which can distinguish between those models. As examples we focused on the obtainable accuracy in the measurement of the W-dependence, the observation of shrinkage and the measurement of the ratio between the longitudinal and the transverse cross section.

For a luminosity of about 250pb^{-1} the measurements with heavy vector mesons are limited by the available statistics. The high luminosity option of HERA is therefore favored. For measurements with the ρ^0 vector meson, and with the heavier vector mesons at very high luminosity, the main systematic uncertainty becomes the estimate of proton dissociation. A very good tagging of the forward proton or proton fragments is needed. Tagging devices sensitive to an angle of 1.5 mrad relative to the proton direction are needed to reduce this error to the level of other uncertainties. It is recommended to have a redundant system of tagging devices with decreasing angular acceptance to be able to study the angular distribution of the proton fragments and to separate scattered protons at large momentum transfers from dissociated protons.

References

[1] M. G. Ryskin, Z. Phys. C57 (1993) 89; M. G. Ryskin *et al.*, HEP-PH 9511228

[2] S. J. Brodsky *et al.*, Phys. Rev. D50 (1994) 3134; L. L. Frankfurt, W. Koepf, M. Strikman, HEP-PH 9509311

[3] J. Nemchik *et al.*, HEP-PH 9605231

[4] J. Bartels *et al.*, Phys. Lett. B375 (1996) 301

[5] A. Donnachie, P. V. Landshoff, Phys. Lett. B185 (1987) 403; Nucl. Phys. B311 (1989) 509

[6] NMC Collaboration, M. Arneodo *et al.*, Z. Phys. C51 (1991) 387

[7] ZEUS Collaboration, M. Derrick *et al.*, Phys. Lett. B356 (1995) 601

[8] H1 Collaboration, S. Aid *et al.*, Nucl. Phys. B468 (1996) 3

[9] M. Glück, E. Reya, A. Vogt, Z. Phys. C67 (1994) 433

[10] M. Arneodo, L. Lamberti, M. G. Ryskin, DESY 96-149

[11] J. R. Forshaw, M. Ryskin, Z. Phys. C68 (1995) 137

[12] UA5 Coll., G. J. Alner *et al.*, Nucl. Phys. B291 (1987) 445

[13] T. Sjöstrand, Comp. Phys. Comm. 82 (1994) 74

[14] A. D. Martin *et al.*, Phys. Rev. D50 (1994) 6734

[15] L. West, to be published

[16] A. Garfagnini, L. Iannotti, L. Lamberti, to be published

[17] T. H. Bauer *et al.*, Rev. Mod. Phys. 50 (1978) 261